

TUNGSTEN-VANADIUM OXIDE SPUTTERED FILMS FOR ELECTROCHROMIC DEVICES

T. Richardson, K. von Rottkay, J. Slack, F. Michalak, M. Rubin

Ernest Orlando Lawrence Berkeley National Laboratory,
Berkeley, CA 94720, USA

ABSTRACT

Mixed vanadium and tungsten oxide films with compositions ranging from 0 to 100% vanadium (metals basis) were prepared by reactive sputtering from metallic vanadium and tungsten targets in an atmosphere of argon and oxygen. The vanadium content varied smoothly with the fraction of total power applied to the vanadium target. Films containing vanadium were more color neutral than pure tungsten oxide films, tending to gray-brown at high V fraction. The electrochromic switching performance of these films was investigated by *in situ* monitoring of their visible transmittance during lithium insertion/extraction cycling in a non-aqueous electrolyte (1M LiClO₄ in PC). The solar transmittance and reflectance was measured ex-situ. Films with vanadium content greater than about 15%, exhibited a marked decrease in switching range. The coloration efficiencies followed a similar trend.

INTRODUCTION

Mixed metal oxides have been investigated for their potential to improve existing electrochromic films. Possible beneficiary effects on the electrochromic host material are increased coloration efficiency, improved durability, color neutrality, a larger switching potential range or faster reaction kinetics. Both Granqvist and Monk (1,2) recently reviewed mixed metal oxides and gave a useful summary. Binary combinations with WO₃ are mentioned with oxides of Ag, Ce, Co, Cr, Cu, Fe, Mo, Nb, Ni, Ru, Sn, Ta, Ti, V and Zn. However, the width of reported combinations by far exceeds the studies' depth.

Even ternary mixtures containing V₂O₅-WO₃ were suggested with additional components of MoO₃ (3), Li₂O (4) and VO₂ (5), but due to the large influence of thin film deposition parameters it may be conjectural to what extent the combined properties are affected by the individual components.

The most cited advantage of V₂O₅-WO₃ is its potential to provide a neutrally coloring electrochromic electrode (3,6,7). In WO₃ the spectral position of the broad absorption

band in the NIR (near infrared spectral region) varies between approximately 1.3 eV for disordered films (8-23) and 0.9 eV for a single-crystalline WO_3 (24). Therefore WO_3 exhibits in either case a characteristic bluish tint in the colored state. This work found the effective absorption band of vanadium (7%) tungsten (93%) oxide blue-shifted by 0.5 eV versus pure WO_3 , hence providing a more neutral color.

From studies on bulk crystals of V_2O_5 - WO_3 they are known to consist of regular blocks of corner-sharing octahedra that are connected by edge-sharing octahedra (25-28). The electrochromic properties of V_2O_5 itself are given in (29-34).

EXPERIMENTAL

Thin film deposition

Films were co-deposited by DC magnetron reactive sputtering using W (99.95%) and V (99.9%) targets. The Ar (99.9995%) flow rate was 220 sccm, delivered into the chamber through the sputter guns, flowing up between the anode shield and the cathode, and then across the target surfaces. The O_2 (99.998%) was delivered through a manifold at the substrate surface. Oxygen flow rates were 50 sccm for the WO_3 and W-V oxides, and 40 sccm for V_2O_5 . Deposition pressure was 30 mTorr. The chamber was pumped with a 450 l/sec LH turbomolecular pump backed by a LH D40B roughing pump. The as-deposited base pressure (i.e. base with turbo throttled to run pressure position) was below 2.0×10^{-6} , with an ultimate system base pressure of less than 7.0×10^{-7} Torr. Two Angstrom Sciences 2" sputter sources inclined 20 degrees off normal to a common focal point were used for co-deposition. The target-to-substrate distance was 17-cm. Compositional variation was achieved using W powers between 15 and 350 Watts, and V powers between 50 and 375 Watts. Total power for the binary metal oxide runs varied between 250 and 575 Watts. Single oxide runs were done at 200 and 200-350 Watts respectively for vanadium and tungsten.

Deposition rates ranged from 16 Å/sec for WO_3 at 350 Watts, down to 0.2 Å/sec for pure V_2O_5 utilizing 200 Watts V power and 40 sccm O_2 . For growth of the mixed oxides with vanadium concentration below 15 %, the most promising range, a rate of 7.5 Å/sec was typical. Rates declined rapidly as the percent of total power contributed by the vanadium source exceeded 70%. The 68 % vanadium concentration run had a rate of 1 Å/sec, with 25 Watts tungsten power and 375 Watts vanadium power. Growth of WO_3 requires substantially higher oxygen pressure than does V_2O_5 . A lower oxygen pressure for the pure V_2O_5 run would have resulted in a much higher deposition rate, but would have been a significant departure from the deposition environment required for the mixed oxide runs. Typical film thickness was between 4400 and 5100 Å for films below 15% V, 2900 to 3000 Å for films with intermediate V concentrations, 2000 to 2300 Å for films over 60% V, and 1500 Å for the pure V_2O_5 film.

Films were deposited onto TEC 15 (SnO_2 :F coated glass) and ITO substrates. Prior to deposition the substrate holder was heated to 120°C with the intention of driving moisture from the substrate surface. Deposition began after the holder had cooled to approximately 50°C. The deposition process maintained the temperature at approximately 50°C for the duration of the run. The discussion of AFM analysis on heated samples is based on a series of

high temperature runs in which the substrate holder (aluminum plate, 8.5 x 8.5 x 0.7 cm) was heated to temperatures ranging between 325°C and 525°C.

The film composition varied smoothly with the ratio of sputtering power applied to the guns as shown on Figure 1. The W/V ratios were determined by RBS, or by PIXE for V concentration lower than 1 at%. The W/O ratios were obtained after fitting the RBS spectra with the appropriate model.

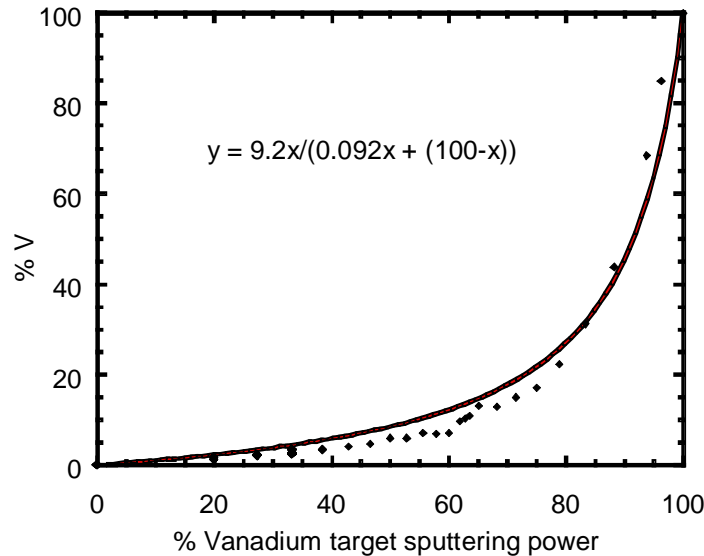


Figure 1. Atomic vanadium fraction in the mixed oxides films as a function of the ratio of sputtering powers $P(V)/[P(W)+P(V)]$

Optical measurements

Optical measurements were made with a variable-angle spectroscopic ellipsometer (VASE) from 280 nm to 1700 nm using an instrument from the J. A. Woollam Co.. Ellipsometric data was taken at three different angles in order to provide data with good signal to noise ratio at each wavelength as well as to over-determine the system of unknown model parameters. To extend the covered spectral range to the whole solar spectrum, transmittance and reflectance measurements from 250 nm to 2500 nm were added; these measurements were taken at near-normal incidence on a Perkin-Elmer Lambda 19 spectrophotometer.

Atomic Force Microscopy

AFM measurements were performed with a Park Scientific M5 instrument. Typical scans were taken over 2 x 2 μm at a scan frequency of 1 Hz. A Si tip was operated at $F = 50$ nN in contact mode. Whole images were corrected for slope in fast and slow scan directions and analyzed without filtering.

Electrochemical cycling

The film samples were transferred to a helium-filled glove box (O_2 and $H_2O < 1$ ppm) in which all electrochemical testing was performed. Lithium insertion and extraction was carried out using an Arbin battery testing system in glass test cells with 1M $LiClO_4$ /propylene carbonate electrolyte and lithium foil counter and reference electrodes. Solar transmittance was measured *in situ* during cycling by means of a fiber optic light source (Oriol) and photometric detectors with appropriate filters (International Light).

RESULTS

Ellipsometric and transmittance data were used to extract the optical constants of the vanadium tungsten oxide films in the range of 280 - 2500 nm. A parametric dispersion model (35,36) assuming a Gaussian broadening was found to fit the data of these amorphous materials more adequately than a Lorentz oscillator model (37). However, reasonable fits were obtained in both cases. The real part of the refractive index at wavelengths longer than in the ultraviolet gradually increases during the transition from WO_3 towards V_2O_5 (Figure 2). The significant scatter of refractive index data in the low vanadium region illustrates the error bars of our deposition process under the same conditions over a period of six months. Among the reasons for the deviations are differences in film thickness and substrate temperature, which was not constrained by external means.

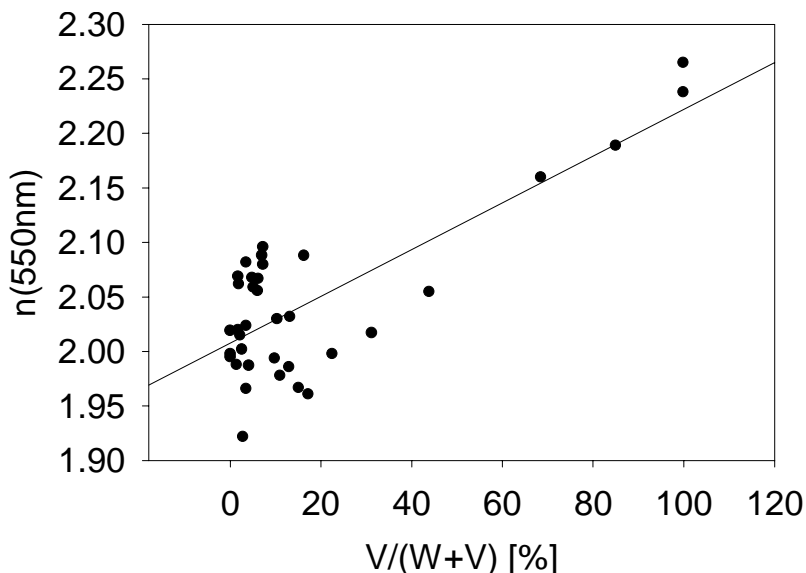


Figure 2. Real part of the refractive index at 550 nm of V-W oxides as a function of vanadium content. The line is drawn for convenience.

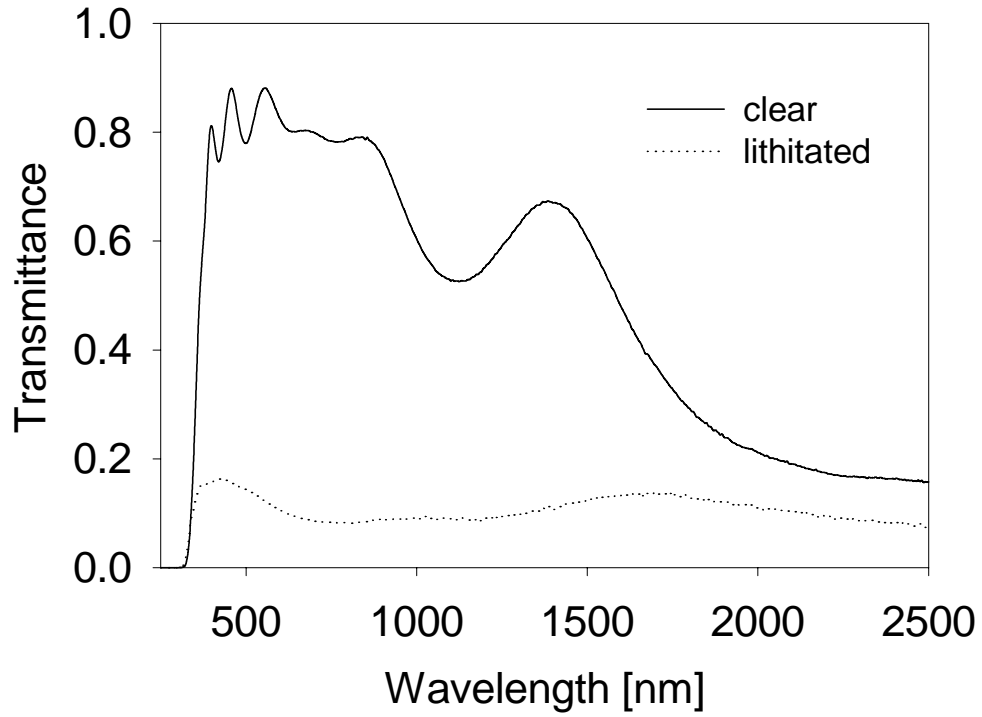


Figure 3. Spectral transmittance of a V-W oxide film with 7% vanadium in clear and dark state.

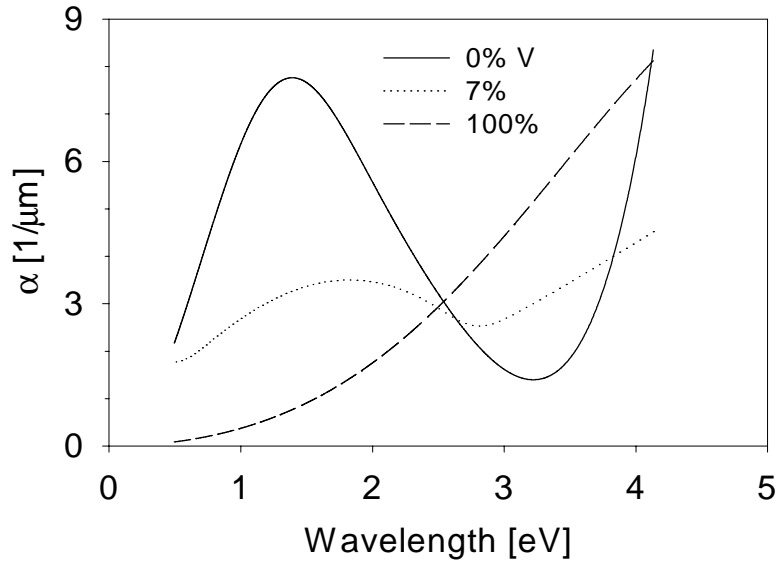


Figure 4. Spectral absorption coefficient for lithiated vanadium tungsten oxides as a function of the atomic vanadium fraction $V/(V+W)$

One clearly sees a blue shift of the absorption peak when adding vanadium to tungsten oxide. The addition of 7% vanadium to tungsten oxide induces a blue shift of the effective absorption peak from 1.3 eV to 1.8 eV, which is responsible for the more

neutral grayish color of vanadium tungsten oxide compared to the typical bluish tint of pure WO_3 .

Because only 7% of vanadium was added to the tungsten oxide, the spectral absorption in the lithiated state does not agree with an effective medium theoretical treatment of the film as a mixture of lithiated WO_3 with lithiated V_2O_5 (30). The reason for the large effect of the small vanadium fraction can be found in the preferential occupation of V3d sites upon lithiation as was reported before (30,38).

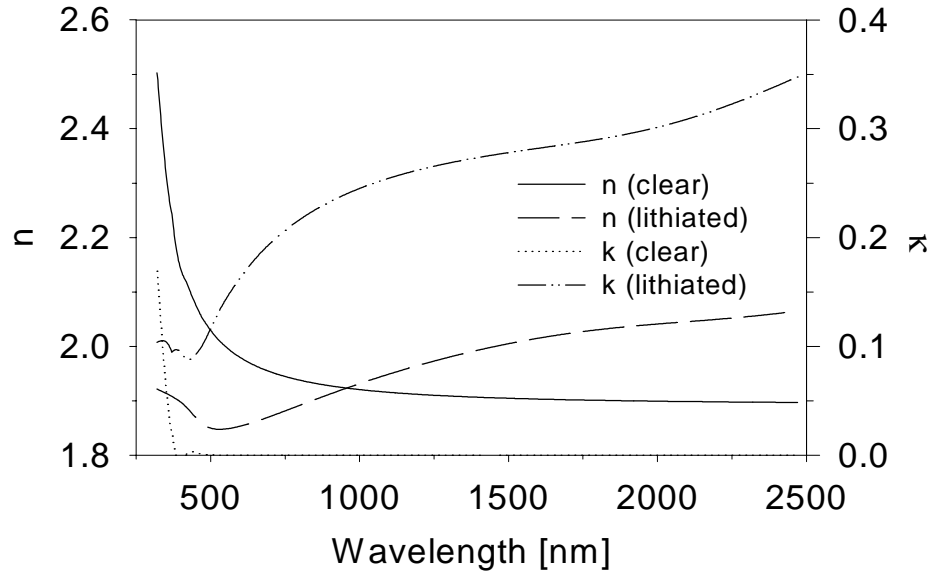


Figure 5. Real and imaginary part of a W-V oxide film with 7% vanadium in clear and lithium intercalated state.

Atomic force microscopy (AFM) was used to determine the root-mean-square roughness of tungsten vanadium oxide films in the low vanadium regime. Disordered films of about 450 nm thickness on ITO substrate were found to have a rather constant surface roughness of about 5 nm. Measurements on crystalline films deposited at 400°C on ITO revealed that a 7% vanadium addition increased the average grain size from 175 nm to 250 nm (Figure 6).

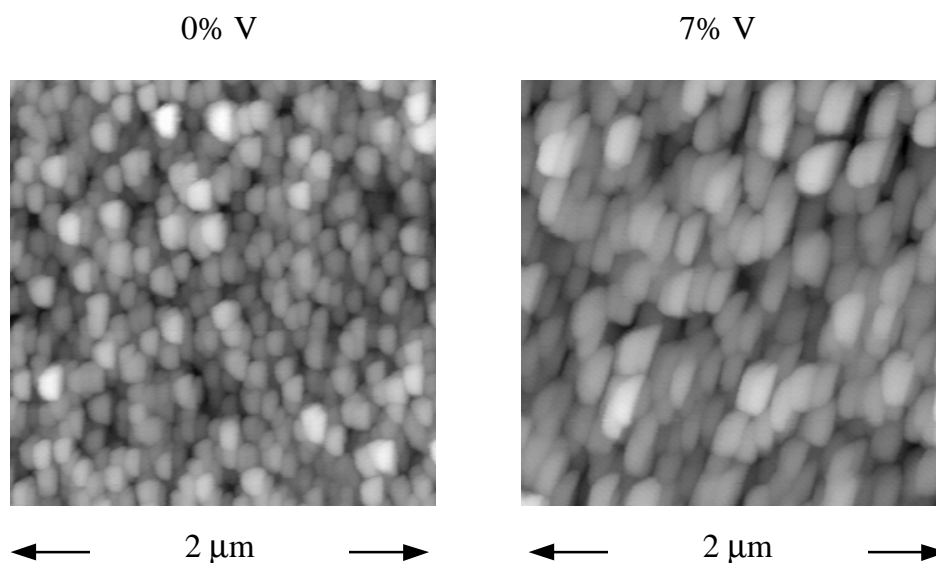


Figure 6. AFM images of tungsten vanadium oxide films on ITO deposited at 400°C, as a function of atomic vanadium fraction

AFM was also used to investigate the effects of post-deposition treatment. WO_3 films post-deposition heat-treated in air were found to degrade rapidly upon electrochemical cycling. Devices based on this material shorted out. Examination by atomic force microscopy revealed cracks in the films as the likely cause for failure leaving the transparent conductor partly exposed to the electrolyte (Figure 7).

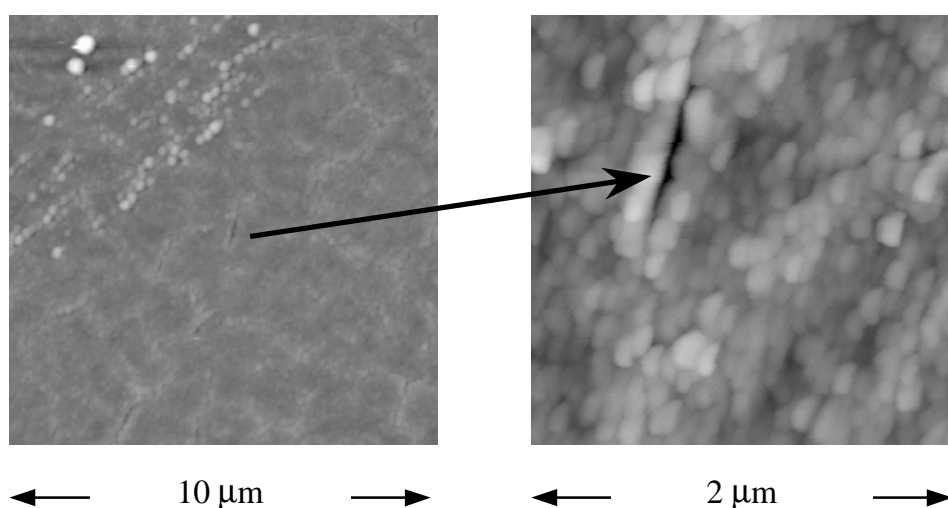


Figure 7. AFM scans of sputtered WO_3 heat-treated at 400°C and electrochemically cycled in LiClO_4 . The line pattern in the 10 μm scan is identified as cracks in the 2 μm scan.

It is interesting to note that similar measurements on films deposited at 400°C did not show any cracks in the surface. Electrochemical cycling of those crystalline films did not result in surface roughening detectable by AFM in contrast to films deposited at room temperature.

The influence of the substrate was significant. About 400 nm thick films of WO_3 deposited at 400°C on ITO resulted in surface roughness in the order of 6 nm, whereas films on TEC15 (essentially $\text{SnO}_2\cdot\text{F}$ (39)), resulted in a roughness of 18 nm. The roughness of the bare substrates was about 3 nm for ITO versus 30 nm for TEC15.

Electrochemical tests

Figure 8, Figure 9 and Figure 10 show the cyclic-voltamograms of a series of tungsten vanadium oxides samples with composition ranging from 0% to 100% Vanadium. For compositions between 0% and 10% vanadium, the CVs look like those of amorphous, pure tungsten oxides thin films. The CVs for vanadium rich samples, i.e. vanadium content higher than 68% look very similar to CVs of pure vanadium oxide sputtered thin films.

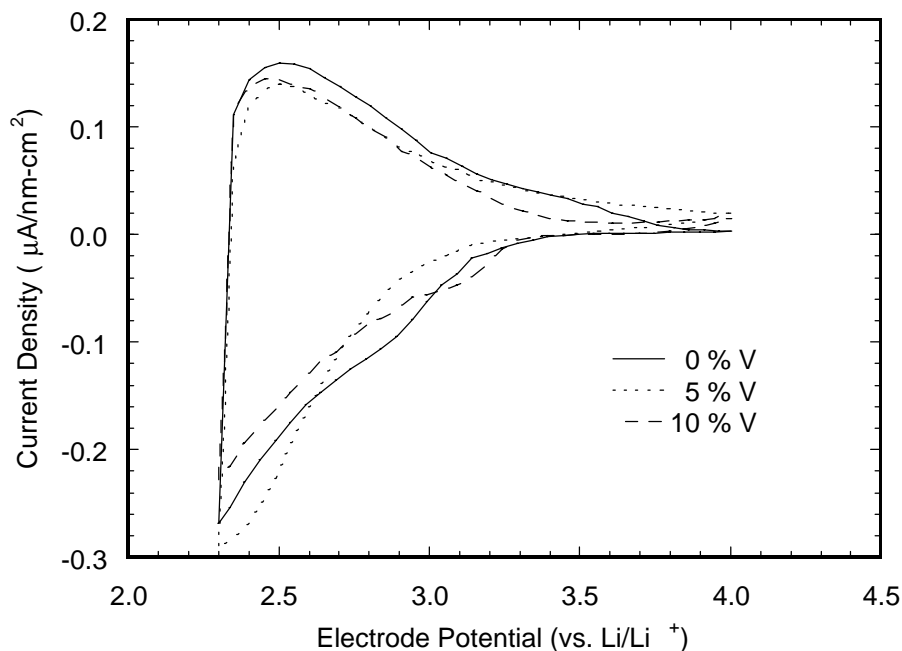


Figure 8: CV of tungsten-vanadium oxide at $2\text{mV}\cdot\text{s}^{-1}$ in PC-1M LiClO_4 , for samples containing 0%, 5% and 10% Vanadium (atom %)

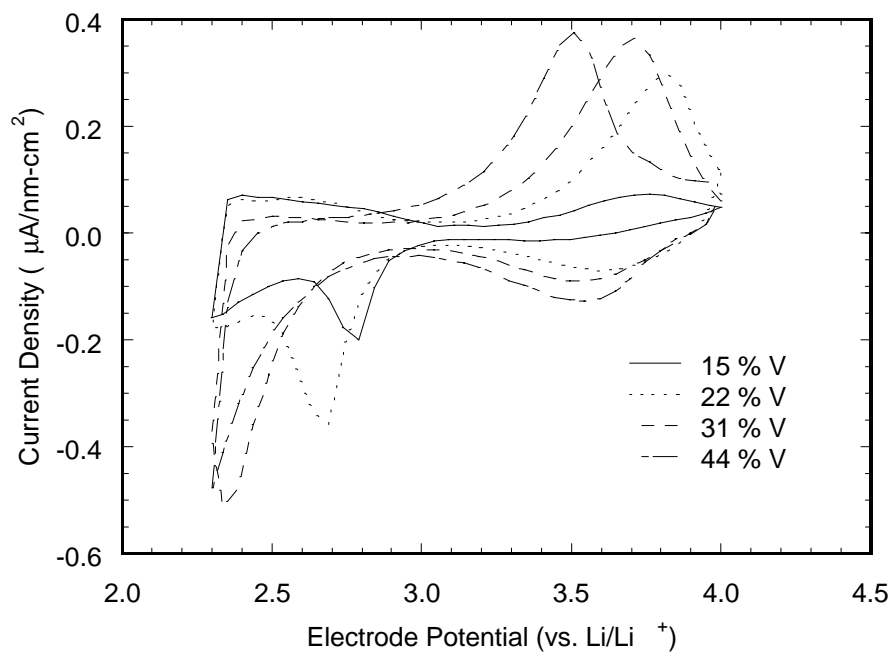


Figure 9: CV of tungsten-vanadium oxide at 2mV.s^{-1} in PC-1M LiClO₄, for samples containing 15%, 22%, 31% and 44% Vanadium (atom %)

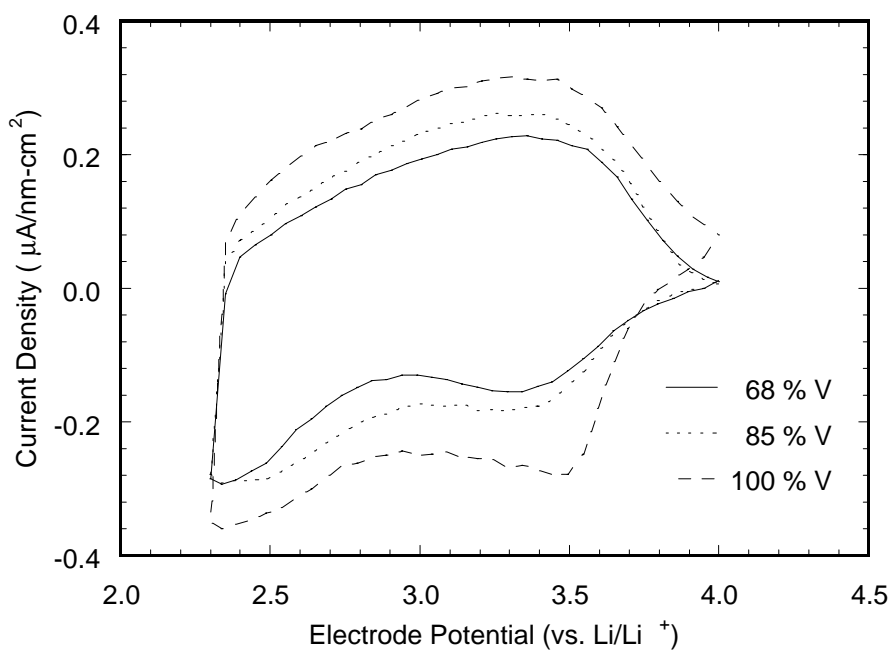


Figure 10: CV of tungsten-vanadium oxide at 2mV.s^{-1} in PC-1M LiClO₄, for samples containing 68%, 85% and 100% Vanadium (atom %)

However, samples with composition between 15% and 44% are very different one to another as shown on Figure 9 and Figure 11.

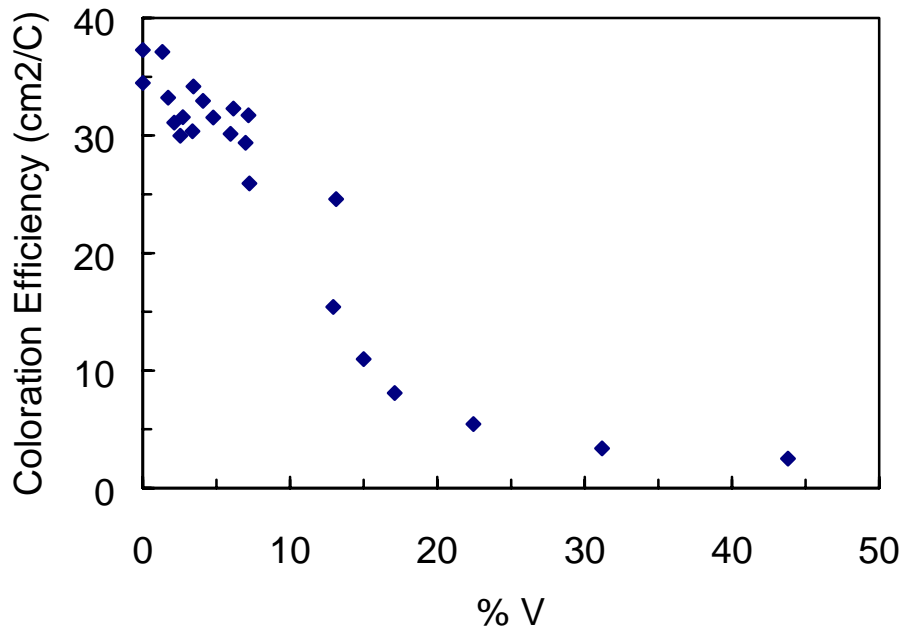


Figure 11. Coloration efficiency (photopic) of W-V oxides as a function of vanadium content.

For this range of composition both the tungsten and the vanadium can be detected in the CV. The optical properties however relate more to those of vanadium oxide, ie low coloration efficiency. For lower vanadium content, ie in the range 0 to 7 at% , the coloration efficiency remains high, between 30 mC.cm^{-2} and 40 mC.cm^{-2} .

CONCLUSION

We deposited mixed tungsten-vanadium oxides by reactive DC magnetron co-sputtering from V and W targets. The composition of these films ranged from 0 to 100% vanadium and was determined by RBS. The composition varied smoothly with the ratio of applied power to the guns.

The absorption band shifted from 1.3eV for a pure tungsten oxide film (0%V) to 1.8 eV for a film containing 7 at% of vanadium (metals basis). The color of this film is more neutral than that of pure tungsten oxide.

The cyclability is good but the coloration efficiency decreases rapidly with V content above 7 at%.

ACKNOWLEDGEMENTS

This work was supported by the Assistant Secretary for Energy Efficiency and Renewable Energy, Office of Building Technologies, Building Systems and Materials Division of the US Department of Energy under Contract No. DE-AC03-76SF00098.

REFERENCES

1. C.G. Granqvist, *Handbook of Inorganic Electrochromic Materials*, Elsevier Science, Amsterdam, 1995, p.225
2. P. M. S. Monk, R. J. Mortimer, D. R. Rosseinsky, *Electrochromism*, VCH, Weinheim, 1995, p.78ff
3. S. Sato, Y. Seino, *Electronics and Communications in Japan*, **65-C**, No.8 (1982) 104
4. W.F. Chu, R. Hartman, V. Leonhard, G. Ganson, *Mat. Sci. Eng.* **B13**, (1992) 235
5. R.J. Cava, D.W. Murphy, S.M. Zahurak, *J. Electrochem. Soc.* **130** (1983) 243
6. S. Huang, J. Zhou, J. Chang, *SPIE* **823** (1987) 159
7. F. Kirino, Y. Ito, K. Miyauchi, T. Kudo, *Nippon Kagaku Kaishi* (1986) 445
8. W.C. Dautremont-Smith, M. Green, K.S. Kang, *Electrochim. Acta* **22** (1977) 751
9. H. Akram, M. Kitao, S. Yamada, *J. Appl. Phys.* **66** (1989) 4364
10. M. Green, Z. Hussain, *J. Appl. Phys.* **69** (1991) 7788
11. F.G.K. Baucke, J.A. Duffy, R.I. Smith, *Thin Solid Films* **186** (1990) 47
12. I.F. Chang, B.L. Gilbert, T.I. Sun, *J. Electrochem. Soc.* **122** (1975) 955
13. R.J. Colton, A.M. Guzman, J.W. Rabelais, *J. Appl. Phys.* **49** (1978) 409
14. A. Donnadieu, D. Davazoglou, A. Abdellaoui, *Thin Solid Films* **164** (1988) 333
15. A. Chemseddine, R. Morineau, J. Livage, *Solid State Ionics* **9-10** (1983) 357
16. S. Hashimoto, H. Matsuoka, *J. Electrochem. Soc.* **138** (1991) 2403
17. F. Kanai, S. Kurita, S. Sugioka, M. Ii, Y. Mita, *J. Electrochem. Soc.* **129** (1982) 2633
18. H. Morita, *J. Appl. Phys.* **24** (1985) 750

19. A. Nakamura, S. Yamada, *Appl. Phys.* **24** (1981) 55
20. P. Schlöter, *Sol. Ener. Mat.* **16** (1987) 39
21. J.S.E.M. Svensson, C.-G. Granqvist, *Sol. Ener. Mat.* **11** (1984) 29
22. T. Yoshimura, M. Watanabe, Y. Koike, K. Kiyota, M. Tanaka, *J. Appl. Phys.* **53** (1982) 7314
23. E.K. Sichel, J.I. Gittleman, J. Zelez, *Appl. Phys. Lett.* **31** (1977) 109
24. E. Salje, *Opt. Commun.* **24** (1978) 231
25. R.J. Cava, D.J. Kleinman, S.M. Zahurak, *Mater. Res. Bull.* **18** (1983) 869
26. G. Heurung, R. Gruehn, *J. Solid State Chem.* **55** (1984) 337
27. G. Heurung, R. Gruehn, *Z. Anorg. Allg. Chem.* **513** (1984) 175
28. J. Ismail, M.F. Ahmed, P.V. Kamath, *J. Power Sources* **41** (1993) 223
29. A. Talledo, C.-G. Granqvist, *J. Appl. Phys.* **77** (1995) 4655
30. K. von Rottkay, N. Özer, M. Rubin, T. Richardson, *Thin Solid Films* **308** (1997) 50
31. S. Kobayashi, H. Sakamoto, F. Kaneko, N. Saito, *Trans. Inst. Electron. Commun. Engr. Japan* **67C** (1984) 397
32. A. Talledo, A.M. Andersson, C.-G. Granqvist, *J. Mater. Res.* **5** (1990) 1253
33. A. Talledo, B. Stjerna, C.-G. Granqvist, *Appl. Phys. Lett.* **65** (1994) 2774
34. K. Nagase, Y. Shimizu, N. Miura, N. Yamazoe, *Appl. Phys. Lett.* **60** (1992) 802
35. C. Herzinger and B. Johs, *Guide to Using WVASE32™*, J.A. Woollam Co., Lincoln, NE, 1996, p. 347
36. C.C. Kim, J.W. Garland, H. Abad, P.M. Racciah, *Physical Review B*, **45** (1992) 11749
37. X.-F. He, *J. Opt. Soc. Am. B*, **14** (1997) 17
38. S. Huang, J. Zhou, J. Chang, *SPIE* **823** (1987) 159
39. K. von Rottkay and M. Rubin, *Mater. Res. Soc. Symp. Proc.* **426** (1996) 449